

## 2,4-Dihydrazino-6-Morpholino-1,3,5-Triazine (DHMT) and 2,4-Dihydrazino-6-Piperidino-1,3,5-Triazine (DHPT) as Promising Corrosion Inhibitors of Steel in Acidic Media

Gamal A. El-Mahdy<sup>1,2,3,\*</sup>, Hessa H. Al-Rasheed<sup>1</sup>, Monirah Al Alshaikh<sup>1</sup>, Hamad A. Al-Lohedan<sup>1,2</sup>, Ayman El-Faham<sup>1,4,\*</sup>

<sup>1</sup>Department of Chemistry, College of Science, King Saud University, P.O. Box 2455, Riyadh 11451, Saudi Arabia.

<sup>2</sup>Surfactants research chair, Department of Chemistry, College of Science, King Saud University, Riyadh 11451, Saudi Arabia.

<sup>3</sup>Chemistry Department, Faculty of Science, Helwan University, Helwan, Egypt.

<sup>4</sup>Chemistry Department, Faculty of Science, Alexandria University, P.O. Box 426, Ibrahimia, 12321 Alexandria, Egypt

\*E-mail: [aelfaham@ksu.edu.sa](mailto:aelfaham@ksu.edu.sa)(A.E.F) & [gamalmah2000@yahoo.com](mailto:gamalmah2000@yahoo.com)(G.A.M)

Received: 11 November 2015 / Accepted: 3 April 2016 / Published: 4 June 2016

---

The effect of the two compounds 2,4-dihydrazino-6-morpholino-1,3,5-Triazine (DHMT) and 2,4-dihydrazino-6-piperidino-1,3,5-triazine (DHPT) for corrosion inhibition of steel in hydrochloric acid solution was investigated using electrochemical techniques. DHMT and DHPT were prepared from cyanuric chloride and completely characterized by IR, <sup>1</sup>H NMR, <sup>13</sup>C NMR, and elemental analysis. The electrochemical results indicated good protection performance of the both tested materials towards the corrosion of steel in the chloride-containing environment. Polarization data indicated that the tested DHMT and DHPT labeled as mixed type inhibitors. Nyquist plots composed of a capacitive loop and its diameter increased with increasing inhibitor concentration. The calculated values of IE from EIS method follow the same trend as those obtained from the polarization results. The results indicated that DHMT and DHPT affects the electrochemical properties of steel surface and promoted an insulating layer and strong modifications in the impedance response. At high concentration (225 ppm and 150 ppm) both showed the same performance, while at low concentration (25 ppm and 75 ppm) DHMT show better performance than DHPT. This behaves due to the presence of the oxygen promotes a better film coating on steel.

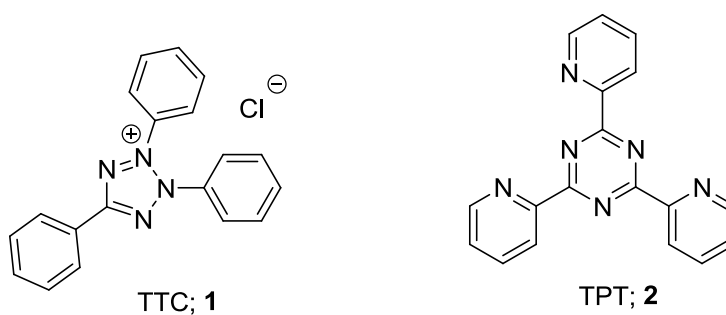
---

**Keywords:** Hydrazino-*s*-triazine, corrosion inhibitors, potentiodynamics polarizatyon, EIS.

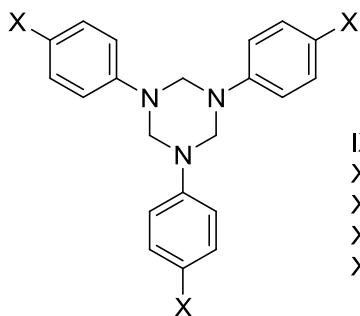
## 1. INTRODUCTION

The study of the steel corrosion phenomena in acidic media has become particularly important because of the increased applications in the industry. Steel is broadly used in industries for acid cleaning, acid descaling of boilers, pickling, heat exchangers, cooling towers, etc. [1,2]. The hydrochloric acid is one of the most broadly agents used. The use of inhibitors is one of the most practical methods for inhibition of corrosion, especially in acidic media. The research in the field of “green” or “eco-friendly” corrosion inhibitors has been addressed toward the objective of using cheap, effective compounds at low or “zero” environmental impact. Significant efforts are deployed to find appropriate compounds to be used as corrosion inhibitors in various corrosive media. A vast number of scientific studies have been dedicated to the subject of corrosion inhibitors for mild steel in acidic media [3–12]. Organic inhibitors generally inhibit the corrosion of the metal by forming a film on the surface of the metal. The efficacy of the inhibitors is dependent on the chemical composition, the molecular structure and their affinities for the metal surface. These materials develop a protecting film on the metal surface, which delivers a barrier to the dissolution of metal in electrolyte solution. The most effective organic inhibitors are compounds having  $\pi$ -bonds in their structures. The adsorption of these compounds are influenced by their electronic structure, steric factor, aromatic character, electron density at donor site, and the presence of functional group such as  $-\text{NH}$ ,  $-\text{N}=\text{N}-$ ,  $-\text{C}=\text{N}$ ,  $-\text{CHO}$ ,  $\text{R}-\text{OH}$  etc.[13-19].

Recently Xuehui *et al.* [20] reported the inhibition effect of 2,3,5-triphenyl-2H-tetrazolium chloride (TTC; **1**) and 2,4,6-tri(2-pyridyl)-s-triazine (TPT; **2**) on the corrosion of mild steel in 1N HCl at room temperature. The results of SEM analysis showed that the metal had been protected from violent corrosion by the addition of **1** and **2**, which resulted in the formation of an adsorption coating film on the surface. TTC (**1**) provided better protection corresponding to those observed in the electrochemical and quantum chemical analyses.

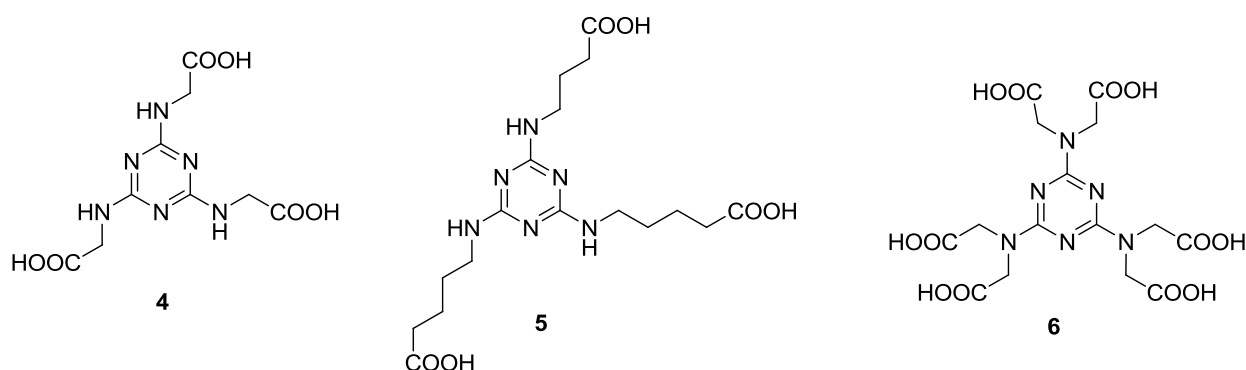


More recently, five-triazine derivatives **3a-e** were synthesized and reported as corrosion inhibitors of mild steel in 1N HCl solution using weight loss, polarization resistance, Tafel polarization and electrochemical Impedance spectroscopy techniques. The inhibiting effect of triazines was found to depend on the electronic nature of the functional groups present in triazines ring [21].



IX= H; Hexahydro-1,3,5-triphenyl-s-triazine ; **3a**  
 X=CH<sub>3</sub>; Hexahydro-1,3,5-p-tolyl-s-triazine; **3b**  
 X= OCH<sub>3</sub>; Hexahydro-1,3,5-p-methoxyphenyl-s-triazine; **3c**  
 X= NH<sub>2</sub>; Hexahydro-1,3,5-p-aminophenyl-s-triazine; **3d**  
 X= NO<sub>2</sub>; Hexahydro-1,3,5-p-nitrophenyl-s-triazine; **3e**

Later Yoo *et al.* [22] reported the corrosion inhibition properties of triazine polycarboxylate **4**, **5**, and **6**. They investigated that the adsorption of the triazine ring enhanced the rust-preventing properties obviously and was the Langmuir isotherm adsorption; the thermodynamic parameters of the adsorption of the triazine derivatives indicated that the adsorption was spontaneous and mainly physisorption.



Herein we reported a new triazine derivatives namely 2, 4-dihydrazino, 6-morpholino-1,3,5-triazine (DHMT) and 2, 4-dihydrazino, 6-piperidino-1,3,5-triazine (DHPT) as a new corrosion inhibitors for steel in M HCl solutions using electrochemical technique.

## 2. EXPERIMENTAL SECTION

### 2.1 Materials

The solvents used were of analytical reagent grade. Cyanuric chloride piperidine, morpholine, and hydrazine hydrates 80% (purchased from Aldrich and used without further purification). The <sup>1</sup>H NMR and <sup>13</sup>C NMR spectra were recorded on a JEOL 400 MHz spectrometer at room temperature. The chemical shifts were measured using internal standard  $\delta = 0$  ppm. Elemental analyses were performed on Perkin-Elmer 2400 elemental analyzer, and the values found were within  $\pm 0.3\%$  of the theoretical values. Melting points were determined with a Mel-Temp apparatus in an open capillary and are uncorrected. The chemical composition, the method of electrode preparation of the working electrode, the reference and the counter electrode are the same as used previously in our studies [23].

## 2.2 General method for the synthesis (DCXT) of 8 and 9

In a 250 mL round bottom flask, a solution of cyanuric chloride **7** (16.59 g, 90 mmol) in 100 mL of acetone was taken and added to a solution of morpholine (7.83g, 90 mmol) or piperidine (7.65 g, 90 mmol) in 100 water at 0 °C followed by addition of NaHCO<sub>3</sub> (7.56 g, 90 mmol) portionwise with stirring at the same temperature. The reaction mixture further stirred at 0°C for 1h. Then ice water was added and the white precipitate was collected by filtration and recrystallized from CH<sub>2</sub>Cl<sub>2</sub>/hexane to afford the desired product

## 2.3. 2, 4-dichloro, 6-morpholino-1,3,5-triazine (DCMT, 8):

The product was obtained as white solid (19.8 g, 94 % yield); mp 157-158 °C [Lit. [24] mp 152-153 °C]. <sup>1</sup>H NMR (CDCl<sub>3</sub>): δ 3.69 (t, 4H, *J* = 5.4 Hz, 2-CH<sub>2</sub>N), δ 3.73 (t, 4H, *J* = 5.4 Hz, 2 - CH<sub>2</sub>O) ppm.

## 2.4. 2,4-dichloro-6-(piperidin-1-yl)-1,3,5-triazine (DCPT; 9):

The product was obtained as a white solid (19.3g, 90% yield); m.p. 76 °C (lit.[25] 72-74 °C); <sup>1</sup>H NMR (CDCl<sub>3</sub>): δ 1.60-1.65 (m, 2H, CH<sub>2</sub>), 1.69-1.72 (m, 4H, 2CH<sub>2</sub>), 3.80 (t, 4H, *J* = 6.1 Hz, 2CH<sub>2</sub>N) ppm.

## 2.5. General method for the synthesis (DHXT)

The solution of DCMT **8** (4.7g, 20 mmol) or DCPT **9** (4.66 g, 20 mmol) in 50 mL acetonitrile was added to a stirred solution of 20 mL hydrazine hydrate (80%) in 50 mL acetonitrile at room temperature. The resulting mixture was stirred under reflux for 3 h, the solvent was removed under reduced pressure and the resulting precipitate was filtered off and washed several times with acetonitrile and then finally with diethyl ether and dried to afford the desired product.

## 2.6. 2, 4-dihydrazino, 6-morpholino-1,3,5-triazine (DHMT,10):

The product was obtained as a white solid in yield 4.3 g (95 %); mp. 215-217 °C; IR (KBr, cm<sup>-1</sup>): 3296, 3199, 1584, 1548, 1497; <sup>1</sup>H NMR (D<sub>2</sub>O-drop TFA): δ 3.42 (brt, 4H, 2×CH<sub>2</sub>N), δ 3.49 (brt, 4H, 2×CH<sub>2</sub>O) ppm; <sup>13</sup>C NMR (D<sub>2</sub>O-drop TFA): δ 44.0, 66.1, 114.7, 117.6, 162.3, 162.9 ppm; Anal. Calcd for C<sub>7</sub>H<sub>14</sub>N<sub>8</sub>O: C, 37.16; H, 6.24; N, 49.53; found: C, 37.38; H, 6.41; N, 49.79.

## 2.7. 2, 4-dihydrazino, 6-morpholino-1,3,5-triazine (DHPT,11):

The product was obtained as a white solid in yield 4.2 g (93 %); m.p 160-162 °C. (lit.[26] 162 °C); IR (KBr, cm<sup>-1</sup>): 3351, 3309, 2926, 1570, 1503, 1506, 1281; <sup>1</sup>H NMR (D<sub>2</sub>O-drop TFA): δ 1.44–

1.59 (6H, m, 3CH<sub>2</sub>); 3.67 (4H, m, 2 CH<sub>2</sub>N) ppm; <sup>13</sup>C NMR (D<sub>2</sub>O-drop TFA): δ 23.5; 25.2; 45.8; 162.8; 163.2 ppm. Anal. Calcd for C<sub>8</sub>H<sub>16</sub>N<sub>8</sub>: C, 42.84; H, 7.19; N, 49.96; found: C, C, 43.06; H, 7.28; N, 49.68.

### 2.8. Electrochemical measurements

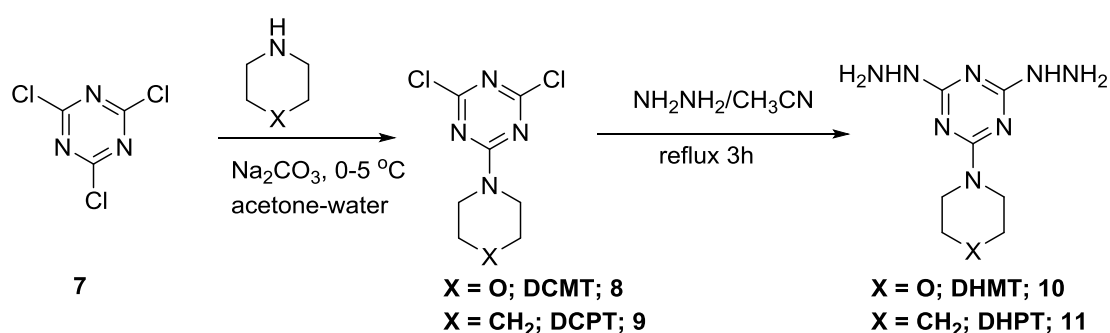
Cathodic, anodic curves and EIS data were conducted using the Solartron 1470E (multichannel system) with the Solartron 1455A as FRA. The polarization curves were recorded with a sweep rate of 1 mV/ s. EIS measurements were measured in the frequency range of 0.01–10 kHz.

## 3. RESULTS AND DISCUSSION

### 3.1. Synthesis of DHXT 10 and 11

The chlorine atoms of cyanuric chloride **7** were replaced first by the amine (morpholine or piperidine), while the second and third chlorine had been replaced by two hydrazine group. Accordingly, 2,4-dihydrazinyl-6-(morpholino-1-yl)-1,3,5-triazine (DHMT, **10**) and 2,4-dihydrazinyl-6-(piperidin-1-yl)-1,3,5-triazine (DHPT, **11**) were prepared by subsequent displacement of chlorine atoms.

First Cyanuric chloride **7** was reacted with the amine at 0 °C for 1h to afford the products **8** and **9** in high yields and purities (Scheme 1). The spectral data were in good agreement with the reported data [24, 26]. The dichloro derivative **8** and **9** was reacted with hydrazine hydrate under reflux using acetonitrile as a solvent to afford the products **10** and **11** (Scheme 1). The spectral data (IR, <sup>1</sup>H NMR and <sup>13</sup>C NMR) proved their structures.



**Scheme 1.** Synthesis of DCXT and DHXT.

### 3.2. Open-circuit potential measurements (OCP)

Figures 1a and 1b represent the dependence of OCP of the steel electrode on concentrations of DHMT (**10**) and DHPT (**11**). The results showed an initial shift in OCP to more negative values with immersion time in the uninhibited and inhibited solutions then slowly and gradually shifts to more

noble values as immersion time elapsed. The initial shift to less noble values can be attributed to the direct attack of the steel surface by the aggressive chloride ions in the medium, which enhances the steel dissolution. As immersion time elapsed, the amount adsorbed DHMT (**10**) and DHPT (**11**) increases and causes a shift in potential to more positive values. In addition, OCP values are highly dependent upon the **10** and **11** concentrations and the shift in OCP values to more noble values increases with increasing **10** and **11** concentrations. The results can be explained based on DHMT (**10**) and DHPT (**11**) adsorption on steel surface.

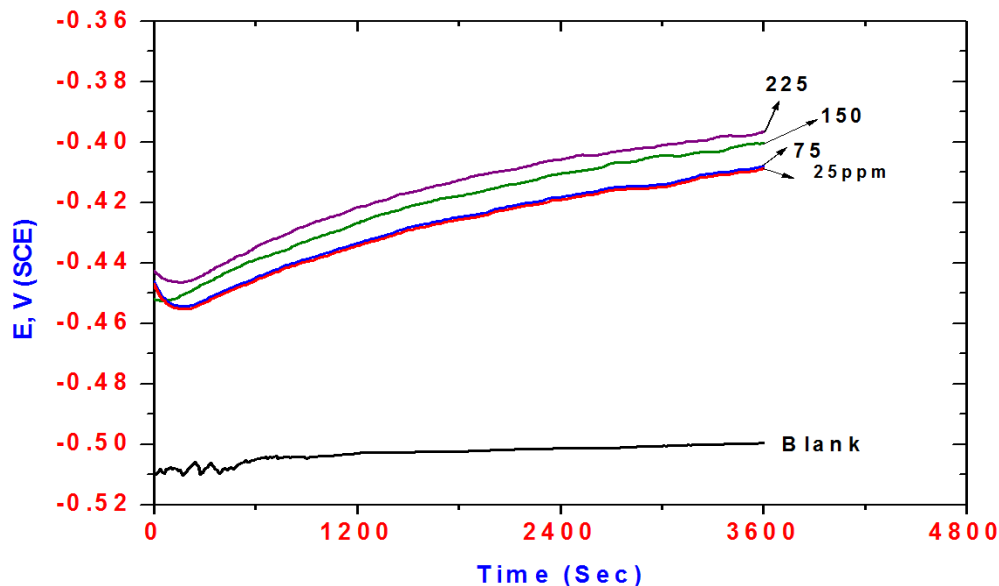


**Figure 1a.** The effect of DHMT concentration on the monitoring data of the open circuit potential of steel in the acidic chloride solution.

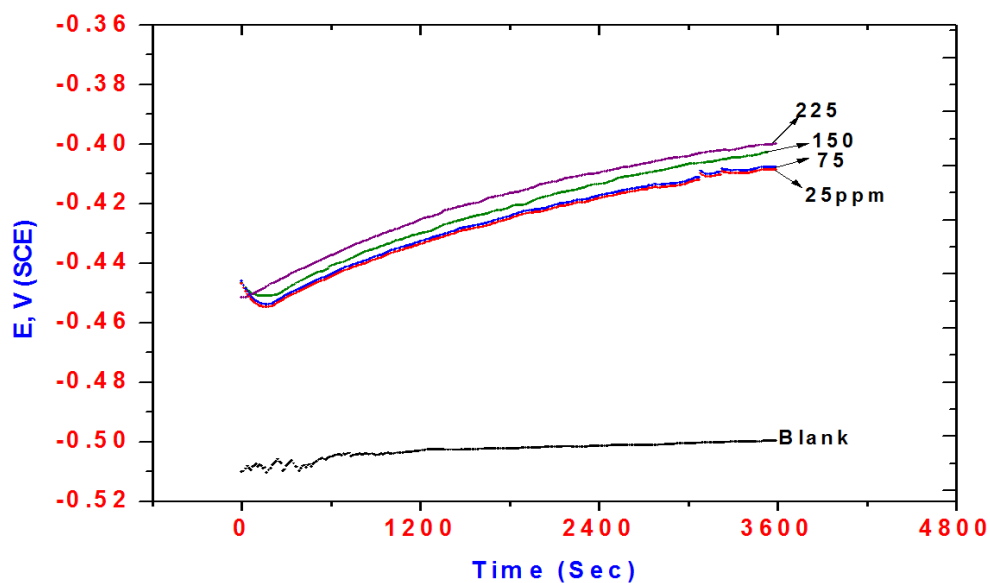


**Figure 1b.** The effect of DHPT concentration on the monitoring data of the open circuit potential of steel in the acidic chloride solution.

3.3. Potentiodynamic polarization measurements

The effect of DHMT (**10**) and DHPT (**11**) concentrations on the polarization curves of steel in acidic chloride solutions are shown in Figures 2a and 2b. A significant reduction in the current density of both branches of the polarization curves was observed. This behavior implies that **10** or **11** displays a high corrosion protection performance and can be labeled as a mixed type inhibitor [27-30]. The addition of **10** or **11** to the acidic chloride solution suppressed both the anodic and cathodic reactions. It is clear that the anodic and cathodic current densities of the inhibited solution containing high DHMT (**10**) or DHPT (**11**) concentration were lowered to small value than that experience by low concentration. It seems that DHMT (**10**) and DHPT (**11**) are adsorbed on anodic and cathodic active sites of the steel surface and thus prevent the anodic and the cathodic reactions. All the estimated electrochemical parameters are given in Table 1. It is expected that the lowering in the values of  $i_{corr}$  in presence of **10** and **11** may be attributed to the adsorption of **10** and **11** on the steel surface by the geometric blocking effect [31].

The results in Table 1 showed that both **10** and **11** gave almost the same results at high concentration (150 and 250 ppm), while DHMT (**11**) gave better results the DHPT (**12**) at low concentration (75 ppm) which indicates that the presence of the oxygen atom in DHMT (**11**) makes it absorbed on the steel surface better than DHPT (**11**).

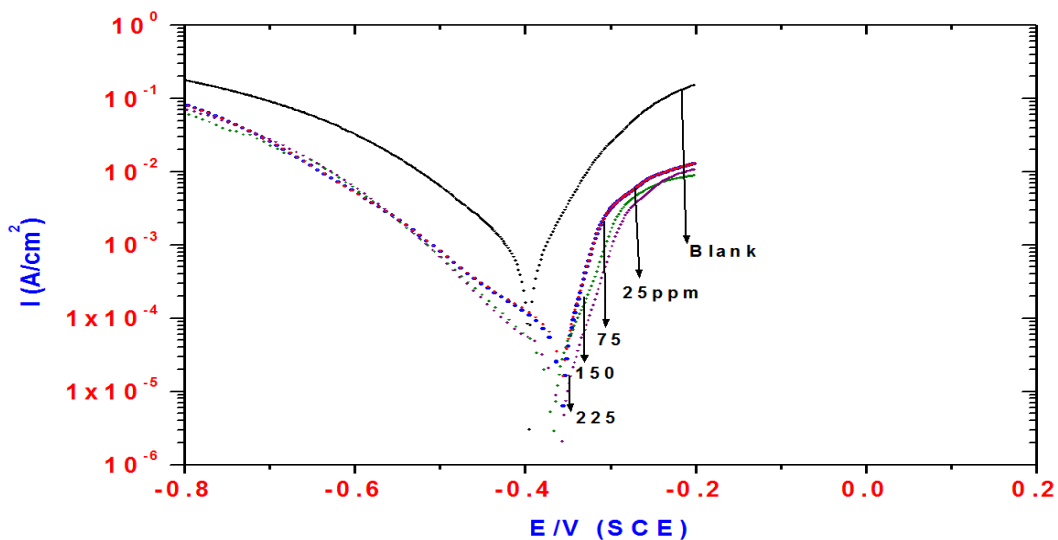


**Figure 2a.** The effect of DHMT concentration on the polarization curves of steel in acidic chloride solutions.

The significant decreases in corrosion current density clearly show the effectiveness of DHMT (**10**) and DHPT (**11**) in inhibiting steel corrosion in HCl solution. The amount of **10** and **11** adsorbed increased with increasing their concentrations. The results can be accounted to more adsorption of **10** and **11** on the steel surface. The inhibition efficiency (IE %) can be computed as [31-33]:

$$IE\% = 1 - i_{corr(inh)} / i_{corr(uninh)}^0 \times 100 \tag{1}$$

Where  $i_{corr(inh)}$  and  $i_{corr}^0$  are corrosion current densities in the inhibited and uninhibited solution, respectively. The dependence of IE% values on DHMT and DHPT concentrations are quoted in Table

1. It is expected that IE% decreased with increasing the concentration of DHMT and DHPT and has a maximum value of IE% (97%) at 225 ppm. The results can be accounted to formation of an inhibitive film, which act as a barrier film for diffusion of the aggressive ions. It can be stated that the presence of DHMT and DHPT suppresses the corrosion rate of steel by the geometric blocking the available active sites on steel surface. Again, The DHMT gave better performance than DHPT at low concentration (75 ppm) 92.2% vs 80.4%, respectively which indicates that the presence of oxygen in DHMT help it to form a better inhibitive film on the steel surface.

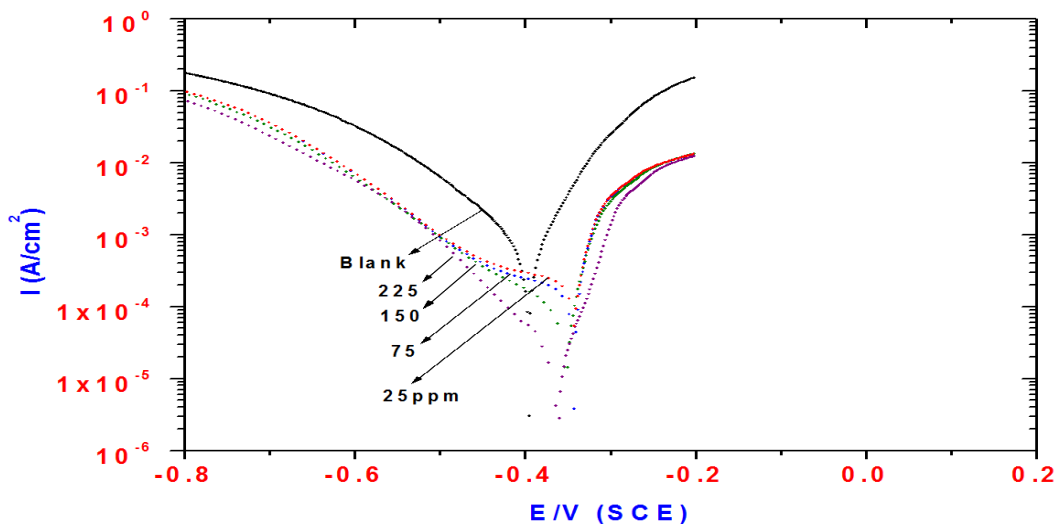


**Figure 2b.** The effect of DHPT concentration on the polarization curves of steel in acidic chloride solutions.

**Table 1.** The effect of DHMT and DHPT concentration on the IE% values for steel in acidic chloride solutions using electrochemical methods.

Polarization Method						EIS Method		
Conc. (ppm)	Ba (mV)	Bc (mV)	E <sub>corr</sub> (V)	i <sub>corr</sub> (μA/cm <sup>2</sup> )	IE%	R <sub>p</sub> (Ohm)	Cdl (μF/cm <sup>2</sup> )	IE%
Blank	69	120	-0.3955	839	-----	1.80	334	-----
DHMT (10)	25	57	-0.3589	73	91	21	109	91.42
	75	59	-0.3584	62	92	23	107	92.17
	150	56	-0.3687	30	96	38	104	95.26
	225	50	-0.3586	19	98	57	101	96.87
DHPT (11)	25	71	-0.3449	174	79	9	137	80.00
	75	66	-0.3443	160	81	9.2	135	80.43
	150	57	-0.3529	47	94	29	105	93.79
	225	51	-0.3628	23	97	56	102	96.78

3.4. EIS studies

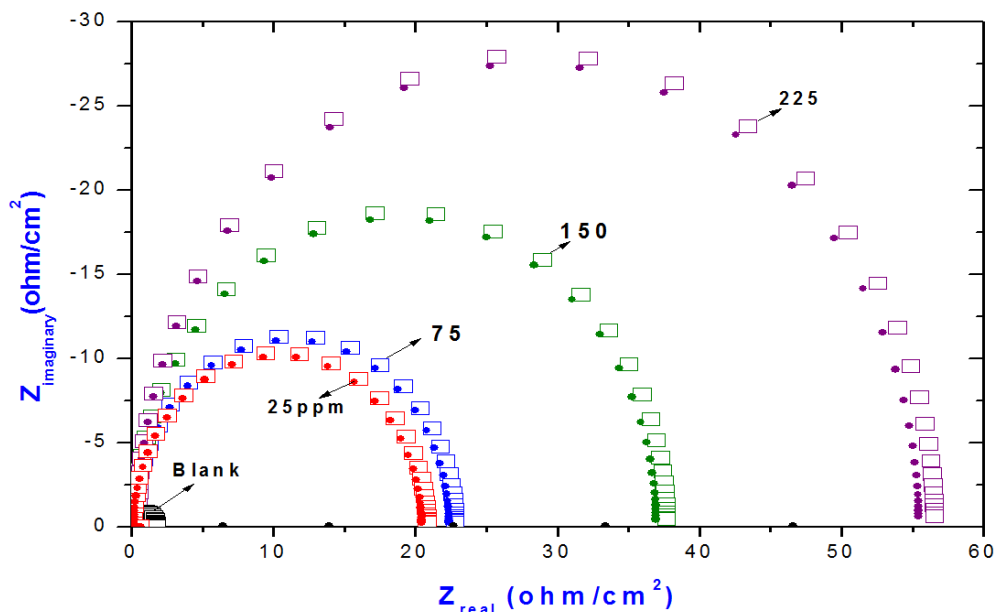


**Figure 3a.** The influence of DHMT concentrations on the the Nyquist plots of steel in acidic chloride solution.

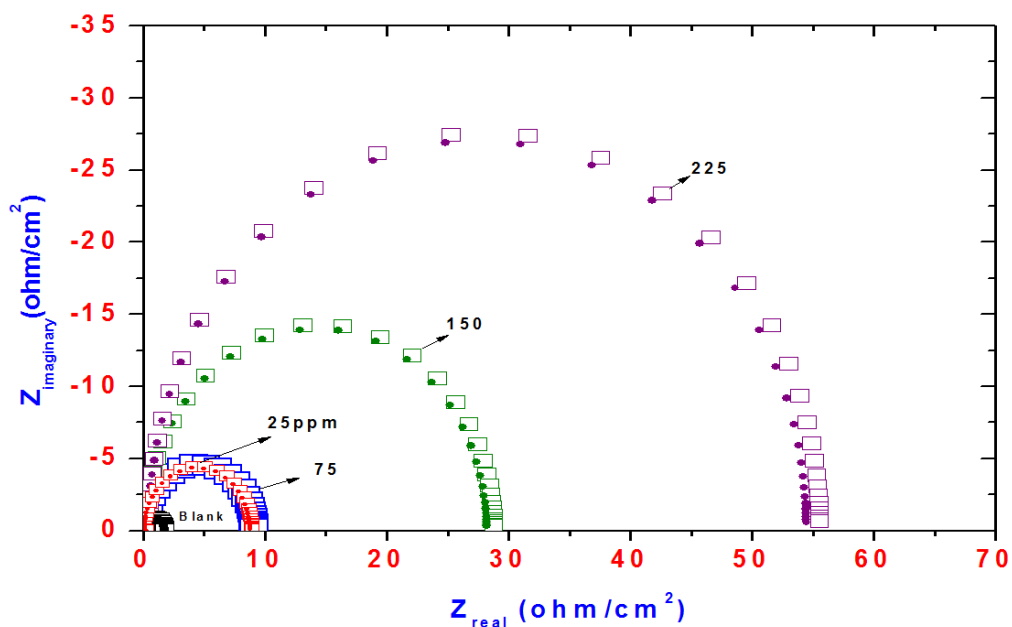


**Figure 3b.** The influence of DHPT concentrations on the the Nyquist plots of steel in acidic chloride solution.

The influence of DHMT and DHPT concentrations on the the Nyquist plots of steel in acidic chloride solution is shown Figure 4a and 4b. The plots composed of one capacitive loop and its diameter increases with increasing DHMT (Figure 3a) and DHPT (Figure 3b) concentration. This

result indicated that DHMT and DHPT have been adsorbed on the steel surface and the amount of adsorbed DHMT and DHPT increased with increasing its concentration.

The processes occurring at the steel/solution interface can be obtained by detailed analysis of impedance spectra using suitably an equivalent circuit shown in Figure 5, which fits the EIS data.  $R_s$  represent the solution resistance, CPE is the constant phase element and  $R_{ct}$  represents the charge transfer resistances. The impedance of the CPE is described as [34-36]:

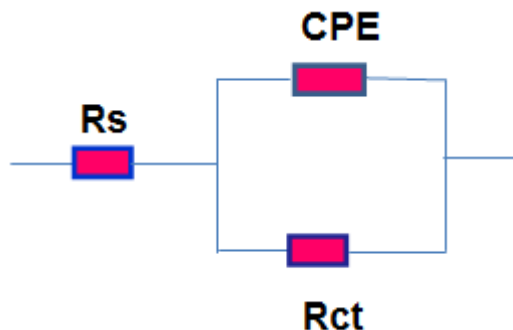


**Figure 4.** Equivalent circuit employed in fitting EIS data.

The same circuit was used in previous studies [23]. It consists of ( $R_s$ ), a constant phase element (CPE) in parallel with ( $R_{ct}$ ). CPE was used instead of Cdl to estimate the EIS data due to heterogeneity and surface roughness [37-39]. The impedance,  $Z_{CPE}$ , are given and expressed as [40-42]:

$$Z_{CPE} = Y_0^{-1} (j\omega)^{-n} \quad (2)$$

Where  $Y_0$  is a proportional factor,  $j^2 = -1$ , and  $\omega$  is the angular frequency ( $\omega = 2\pi f$ ). The factor  $n$  determines the significant of the parameters in the circuit. When  $n \neq 1$  the investigated system may be attributed to the surface heterogeneity [43] or to the charge-transfer reactions [44-48]. The impedance is corresponding to pure capacitance when  $n = 1$ . It is clear that Cdl and  $R_{ct}$  have an opposite trend with each other. The increase in  $R_{ct}$  value with increasing inhibitor concentration can be attributed to the adsorption of DHMT (**11**) and DHPT (**12**) on steel surface. It was established that  $R_{ct}$  is inversely proportional to the corrosion rate and consequently corrosion protection performance. The higher the  $R_{ct}$  value is, the greater the corrosion protection performance of the tested material. The addition of DHMT or DHPT to the aggressive solution is accompanied by a decrease in double layer capacitance. DHMT and DHPT molecules were adsorbed on the steel surface by displacement of the adsorbed water molecules from the surface [49-54]. This in turn blocked the active sites on the surface with a formation of an inhibitive and insulating layer, which hinder the diffusion of the aggressive ions. The IE% was calculated as [55]:

$$IE\% = 1 - R_{ct(1)} / R_{ct(2)} \times 100 \quad (3)$$

Where,  $R_{ct(1)}$  and  $R_{ct(2)}$  are the charge transfer resistances in uninhibited and inhibited solution, respectively. The influence of DHMT and DHPT concentrations on the values of IE% are quoted in Table 1 and it showed that %IE significantly increases with increasing DHMT and DHPT concentrations. The calculated values of IE from EIS method follow the same trend as those obtained from the polarization results.

3.5. Adsorption isotherm

Two types of adsorptions occur through adsorption processes of DHMT and DHPT molecules on the steel surface. Physical adsorption associates with the electrostatic attraction between electrically charged exposed surface and charged ions in the bulk solution. Chemisorption arises from the charge transfer or charge sharing from the adsorbed DHMT and DHPT molecules to the surface of steel. The interaction between the adsorbed DHMT or DHPT molecules and the steel surface is provided by studying the various adsorption isotherm models. The fitting results of the experimental data showed that Langmuir isotherm is the best fit among the other isotherms based on the correlation coefficient,  $R^2$  (0.999) and can be described as [56]:

$$C_{(inh)} / \theta = 1/K_{ads} + C_{(inh)} \tag{4}$$

Where,  $C_{(inh)}$  is inhibitor concentration and  $K_{ads}$  is the equilibrium constant for the adsorption process. The linear plot of  $C/\theta$  versus  $C$  shown in Figure 6a and 6b clearly indicated that the adsorbed molecules of DHMT and DHPT on the steel surface follows the Langmuir isotherm as presented in Figure 6a and 6b with a slope close to unity (0.999). The relation between equilibrium constant of adsorption  $K_{ads}$  and the standard free energy of adsorption ( $\Delta G^{\circ}_{ads}$ ) can be given by the following equation [57,58]:

$$\Delta G^{\circ}_{ads} = -RT \ln (55.5K_{ads}) \tag{5}$$

The computed value of  $\Delta G^{\circ}_{ads}$  on steel was  $-40.74 \text{ kJ mol}^{-1}$  and  $-38.03 \text{ kJ mol}^{-1}$  for DHMT and DHPT, respectively. Generally, the values of  $\Delta G^{\circ}_{ads}$  up to  $-20 \text{ kJ mol}^{-1}$  were considered as physical adsorption, while chemisorption is around  $-40 \text{ kJ mol}^{-1}$  [59,60]. Therefore, the high negative values of  $\Delta G_{ads}$  indicate that the adsorption of DHMT and DHPT on steel might be a combination of both physisorption and chemisorption.

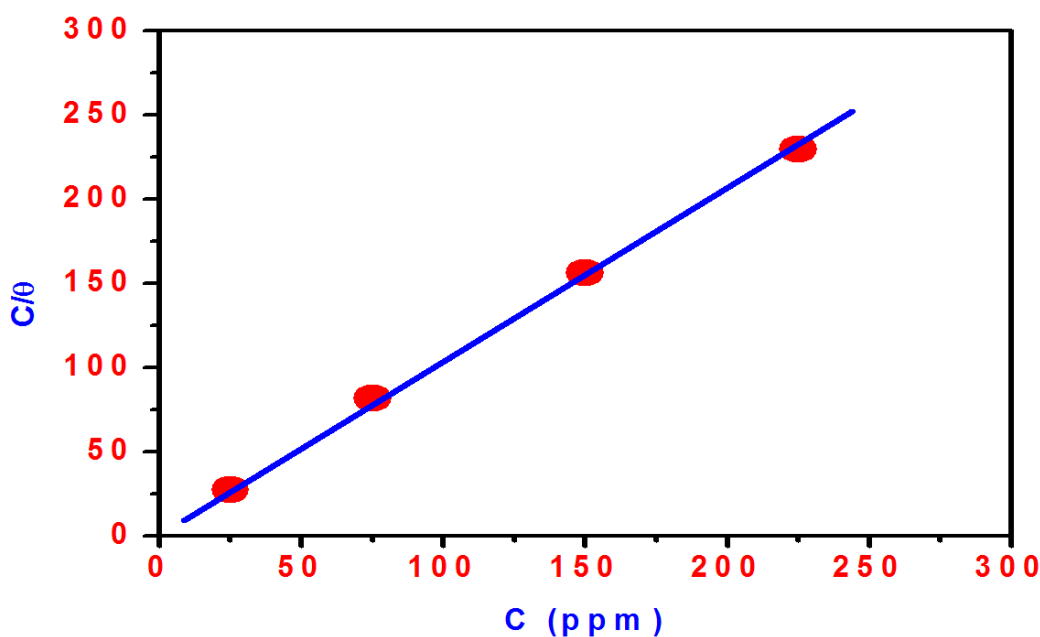
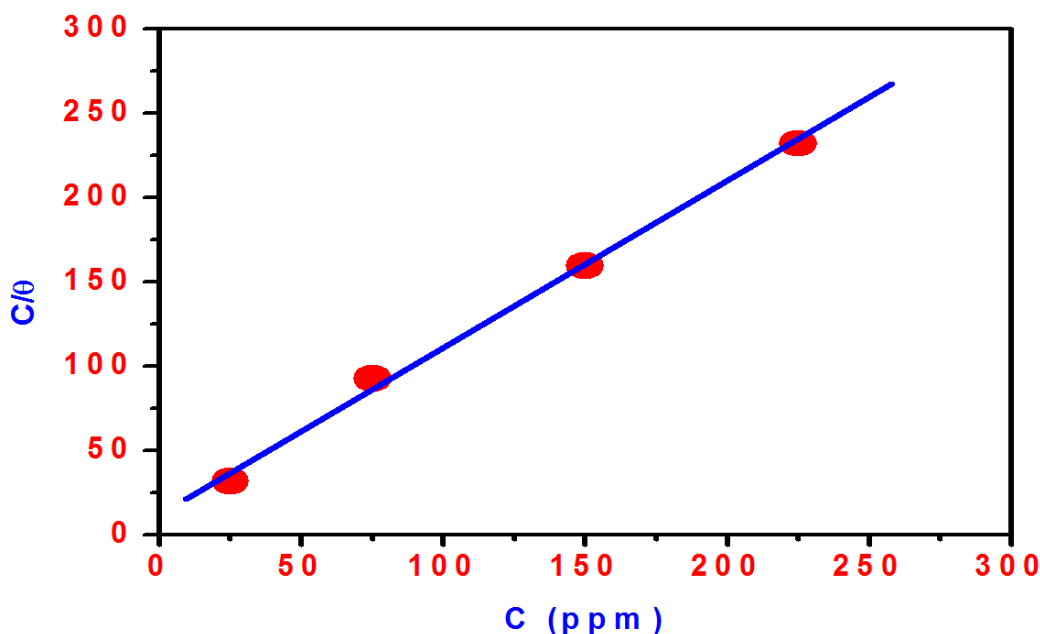


Figure 5a. Langmuir’s isotherm adsorption model of DHMT on steel surface in 1 M HCl solution.



**Figure 5b.** Langmuir's isotherm adsorption model of DHPT on steel surface in 1 M HCl solution.

#### 4. CONCLUSIONS

- 2, 4-Dihydrazino-6-morpholino-1,3,5-triazine (DHMT) and 2,4-dihydrazino-6-piperdino-1,3,5-triazine (DHPT) displayed an excellent inhibitive properties towards the corrosion of steel in the acidic chloride containing solution solutions.
- The inhibitive effect increased by increasing the concentration of the investigated 2, 4-dihydrazino-6-morpholino-1,3,5-triazine (DHMT) and 2,4-dihydrazino-6-piperdino-1,3,5-triazine (DHPT).
- Polarization data revealed that the studied DHMT and DHPT can be labeled as mixed type inhibitors
- The corrosion inhibition of DHMT and DHPT can be interpreted by the geometric blocking of the available active sites on steel surface.
- EIS data indicated that the higher the  $R_{ct}$  value is, the greater the corrosion protection performance of the investigated DHMT and DHPT.
- The calculated values of IE from EIS method follow the same trend as those obtained from the polarization results.
- The adsorption of DHMT and DHPT on steel occurs via physisorption and chemisorptions.
- The presence of the oxygen atom in DHMT increase its performance than DHPT for corrosion inhibition at low concentration (25 ppm and 75 ppm), while both DHMT and DHPT has the same performance at high concentration (150 ppm and 250 ppm)

#### ACKNOWLEDGMENTS

This project was financially supported by King Saud University, Vice Deanship of Research Chairs.

**References**

1. M. S. Abdallaha, O. Al Karanee, A.A. Abdel Fataha, *Chem. Eng. Comm.* 197 (2010) 1446.
2. G. L. Scattergood, Corrosion inhibitors for crude oil refineries, corrosion, AS Handbook, vol. 13, ASM International, 1992
3. P. C. Okafor, Y.G. Zheng, *Corros. Sci.* 51 (2009) 850.
4. P. C. Okafor, X. Liu, Y.G. Zheng, *Corros. Sci.* 51 (2009) 761.
5. Z. Zhang, S. Chen, Y. Li, S. Li, L. Wang, *Corros. Sci.* 51 (2009) 291.
6. M. Mahdavian, M.M. Attar, *Corros. Sci.* 51 (2009) 409.
7. X. Liu, P.C. Okafor, Y.G. Zheng, *Corros. Sci.* 51 (2009) 744.
8. T. Arslan, F. Kandemirli, E.E. Ebenso, I. Love, H. *Corros. Sci.* 51 (2009) 35.
9. F. G. Liu, M. Du, J. Zhang, M. Qiu, *Corros. Sci.* 51 (2009) 102.
10. J. M. Roque, T. Pandiyan, J. Cruz, E. G.Ochoa, *Corros. Sci.* 50 (2008) 614.
11. Z. Ait Chikh, D. Chebabe, A. Dermaj, N. Hajjaji, A. Srhiri, M.F. Montemor, M. G. S. Ferreira, A. C. Bastos, *Corros. Sci.* 47 (2005) 447.
12. A. Rauscher, G. Kutsan, Z. Lukacs, *Corros. Sci.* 35 (1993) 1425.
13. K. Singh, M. A. Quraishi, *Corros. Sci.* 52 (2010) 152
14. I. Lukovits, E. Kalman, G. Palinkas, *Corrosion*, 51 (1995) 201.
15. R. C. Ayers Jr, N. Hackerman, *J. Electrochem. Soc.*, 110 (1963) 507.
16. S. K. Shukla, M.A. Quraishi, R. Prakash, *Corros. Sci.*, 50 (2008) 2867.
17. M. A. Quraishi, S.K. Shukla, *Mater. Chem. Phys.*, 113 (2009) 685.
18. S. K. Shukla, A.K. Singh, I. Ahamad, M.A. Quraishi, *Mater. Lett.*, 63 (2009) 819.
19. A. A. Al-Amiery, A. A. H. Kadhum, A. H. M. Alobaidy, A. B. Mohamad, P. S. Hoon, *Materials*, 7 (2014) 662 .
20. P. Xuehui, H. Baorong, L. Weihua, L. Faqian, Y. Zhigang, *Chin. J. Chem. Eng.*, 15 (2007) 909.
21. S. K. Shukla, A. K. Singh, M. A. Quraishi, *Int. J. Electrochem. Sci.*, 7 (2012) 3371.
22. S-H. Yoo, Y-W. Kim, K. Chung, N-K. Kim, J-S. Kim, *Ind. Eng. Chem. Res.*, 52 (2013) 10880.
23. Ayman M. Atta, G. A. EL-Mahdy, Hamad A. Al-Lohedan and Kamel R. Shoueir, *Int. J. Electrochem. Sci.*, 10 (2015) 870.
24. V. V. Bakharev, A. A. Gidasov, V. E. Parenov, I. V. Ulyankina, A. V. Zavodskaya, E. V. Selezneva, K. Y. Suponitskii, A. B. Sheremetev, *Russian Chem. Bull., Int. Ed.*, 61(2012) 99.
25. T. Peppel and M. Kockerling, *J. Coord. Chem.*, 62 (2009) 1902.
26. W. Huang, W. Zheng, D. J. Urban, J. Inglese, E. Sidransky, Ch. P. Austina, C. J. Thomasa, *Bioorg. Med. Chem. Lett.*, 17 (2007) 5783.
27. M. Finsgar, *Corros. Sci.*, 72 (2013) 82.
28. A. El Bribri, M. Tabyaoui, B. Tabyaoui, H. El Attari, F. Bentiss, *Mater. Chem. Phys.* 141 (2013) 240.
29. M. A. Abu-Dalo, N.A.F. Al-Rawashdeh, A. Ababneh, *Desalination* 313 (2013) 105.
30. F. Bentiss, M. Lebrini, M. Lagrenée, *Corros. Sci.*, 47 (2005) 2915.
31. X. Li, S. Deng, H. Fu, G. Mu, *Corros. Sci.*, 51 (2009) 620.
32. Aljourani, K. Raeissi, M.A. Golozar, *Corros. Sci.*, 51 (2009) 1836.
33. Ahamad, R. Prasad, M.A. Quraishi, *Corros. Sci.*, 52 (2010) 3033.
34. H. Ashassi-Sorkhabi, B. Shaabani, D. Seifzadeh, *Electrochim. Acta* 50 (2005) 3446.
35. M. Tourabi, K. Nohair, M. Traisnel, C. Jama, F. Bentiss, *Corros. Sci.*, 75 (2013) 123.
36. Xu, Y. Liu, X. Yin, W. Yang, Y. Chen, *Corros. Sci.*, 74 (2013) 206.
37. R. M. Carranza, M.G. Alvarez, *Corros. Sci.* 38 (1996) 909.
38. A. S. Ries, M. Da Cunha Belo, M.G.S. Ferreira, I.L. Muller, *Corros. Sci.*, 50 (2008) 968.
39. T. K. Rout, *Corros. Sci.*, 49 (2007) 794.
40. Ahamad, R. Prasad, M.A. Quraishi, *Corros. Sci.*, 52 (2010) 3033.
41. Ahamad, R. Prasad, M.A. Quraishi, *Mater. Chem. Phys.*, 124 (2010) 1155.

42. N. Labjar, M. Lebrini, F. Bentiss, N.E. Chihib, S. El Hajjaji, C. Jama, *Mater. Chem. Phys.* 119 (2010) 330.
43. Z. Lukacs, *J. Electroanal. Chem.*, 464 (1999) 68.
44. J.R. Macdonald, *J. Electroanal. Chem.*, 378 (1994) 17.
45. J.R. Macdonald, *J. Appl. Phys.*, 58 (1985) 1971.
46. J.R. Macdonald, *J. Appl. Phys.*, 58 (1985) 1955.
47. J.R. Macdonald, *J. Appl. Phys.*, 62 (1987) 51.
48. R.L. Hurt, J.R. Macdonald, *Sol. St. Ion.*, 20 (1986) 111.
49. Hosseini, H. Tavakoli, T. Shahrabi, *J. Appl. Electrochem.* 38 (2008) 1629.
50. Lebrini, M. Lagrenee, H. Vezin, L. Gengembre, F. Bentiss, *Corros. Sci.*, 47 (2005) 485.
51. F. S. de Souza, A. Spinelli, *Corros. Sci.*, 51 (2009) 642.
52. M.A. Amin, S. S. Abd El-Rehim, E.E.F. El-Sherbini, R.S. Bayoumi, *Electrochim. Acta* 52 (2007) 3588.
53. E. McCafferty, N. Hackerman, *J. Electrochem. Soc.*, 119 (1972) 146.
54. L. A. S. Ries, M. Da Cunha Belo, M.G.S. Ferreira, I.L. Muller, *Corros. Sci.*, 50 (2008) 968.
55. K. Es-Salah, M. Keddou, K. Rahmouni, A. Srhiri, H. Takenouti, *Electrochim. Acta* 49 (2004) 2771.
56. Ahamad, R. Prasad, M.A. Quraishi, *Corros. Sci.* 52 (2010) 933.
57. E. A. Noor, A.H. Al-Moubaraki, *Mater. Chem. Phys.* 110 (2008) 145.
58. Ozcan, R. Solmaz, G. Kardas, I. Dehri, *Colloids Surf. A* 325 (2008) 57.
59. M. Goulart, A. Esteves-Souza, C.A. Martinez-Huitle, C.J.F. Rodrigues, M.A.M. Maciel, A. Echevarria, *Corros. Sci.* 67 (2013) 281.
60. H. Keles, M. Keles, I. Dehri, O. Serindag, *Mater. Chem. Phys.* 112 (2008) 173.